coatings

MDPI

Communication

Fabrication and Properties of Epitaxial VO_2 Thin Film on m-Al_2O_3 Substrate

Manish Kumar *, Sunita Rani and Hyun Hwi Lee *

Pohang Accelerator Laboratory, Pohang University of Science and Technology (POSTECH), Pohang 37673, Republic of Korea

* Correspondence: manish@postech.ac.kr (M.K.); hhleec@postech.ac.kr (H.H.L.)

Abstract: A thin film of thermochromic VO_2 was prepared on m-Al_2O_3 substrate using a radio frequency (RF) magnetron sputtering technique. The epitaxial growth of the monoclinic M_1 phase of VO_2 on the m-Al_2O_3 substrate was confirmed through synchrotron X-ray diffraction (XRD) measurements. The transformation of this monoclinic M1 phase into a rutile phase at ~68 °C was reflected in the temperature-dependent XRD measurements of the VO_2 thin film. The temperature-dependent electrical resistance measurements of this sample also revealed an abrupt metal-to-insulator transition at ~68 °C, which is reversible in nature. Temperature-dependent X-ray absorption (XAS) measurements at V *L*-edge and O *K*-edge were performed to study the electronic structure of the epitaxial VO_2/m-Al_2O_3 thin film during the metal-to-insulator (MIT) transition.

Keywords: thin film; phase transition; vanadium dioxide

Citation: Kumar, M.; Rani, S.; Lee, H.H. Fabrication and Properties of Epitaxial VO_2 Thin Film on m-Al_2O_3 Substrate. *Coatings* **2023**, *13*, 439. https://doi.org/10.3390/coatings13020439

Academic Editor: Andrey V. Osipov

Received: 6 January 2023
Revised: 31 January 2023
Accepted: 12 February 2023
Published: 15 February 2023

1. Introduction

In recent years, vanadium oxide compounds have been the focus of attention because of their rich fundamental physics and the potential for device applications [1–4]. Among these, the monoclinic M_1 phase of vanadium dioxide (VO_2) is particularly attractive, owing to its dramatic change in physical properties exhibited during phase transition [5,6]. It undergoes metal-to-insulator transition (MIT), along with structural phase transition at a critical temperature (T_C) of ~68 °C [1,7]. VO_2 transforms from a low temperature monoclinic insulating phase into a metallic rutile phase at high temperatures through a first-order phase transition [8]. Below T_C, the insulator phase is transparent to near infra-red (NIR) rays, while above the T_C, it is opaque to NIR rays [6,8]. In addition to thermal activation, the phase transition in VO_2 can be triggered by electrical, optical, and mechanical excitations. Because of these unique features, VO_2 has spurred diverse application in many areas including optical switches, smart windows, Mott memories, THz devices, or field effect transistors [1,9–11]. From the device perspective, it is imperative to grow high-quality thin film VO_2. This is the reason why the researchers have been continuously striving to determine the most viable and optimized method for synthesizing high-quality thin films of VO_2 since the phase transition was first observed in this material. The synthesis of phase-controlled stochiometric VO_2 thin films is slightly tricky as a small variation in the oxygen content can lead to several other compounds of vanadium oxide [12]. Moreover, VO_2 itself can exist in several polymorphs [12]. So, the phase-specific growth of VO_2 thin film with the desired orientation is challenging. The epitaxial growth of VO_2 thin films is desired to realize the single crystal-like properties for device applications. Until now, researchers have widely studied the epitaxial growth of VO_2 thin films mainly on substrates such as c-Al_2O_3 and TiO_2, but studies focused on the epitaxial growth of VO_2 films on m-Al_2O_3 substrates are limited [12–15]. This warrants the study of the fabrication and comprehensive characterization of epitaxial VO_2 thin film prepared on other substrates to achieve the desired orientation and/or properties. Recently, the MIT performance was studied in epitaxial VO_2 thin film prepared on an m-Al_2O_3 substrate using the moisture

assisted chemical solution approach [16]. Zhao et al. reported mixed-orientation growth of VO_2 film on an m-Al_2O_3 substrate by using a sputtering technique [14]. Recently Choi et al. successfully grew epitaxial VO_2 film on an m-Al_2O_3 substrate by using RF sputtering, but the roughness (16.5 nm) of their sample is on the slightly higher side [15].

In the present work, we have stabilized epitaxial VO_2 thin film on m-Al_2O_3 using the RF magnetron sputtering technique and investigated its temperature-dependent structural, electrical, and electronic properties. The detailed study of the structural, electrical, and electronic properties of epitaxial VO_2 thin films is significant in order to achieve device realization and the control of the functionalities of VO_2 thin films.

2. Materials and Methods

Thin films of VO_2 were prepared by means of an RF magnetron sputtering technique using a commercially purchased VO_2 target (Crystal Bank at Pusan National University, Busan, South Korea) with a diameter of 76.2 mm and a thickness of 3 mm. A chemically cleaned m-Al_2O_3 ($10\bar{1}0$) substrate was mounted in the deposition chamber. After achieving the base pressure of 1×10^{-6} Torr in the deposition chamber, the VO_2 target was pre-sputtered for 5 min to clean its surface before the actual deposition. During the deposition, the chamber pressure and substrate temperature were kept at ~0.5 mTorr and ~50 °C, respectively. Ar gas was used for plasma, and the sputtering power was maintained at 200 W. This was followed by the external annealing of a grown sample in a rapid thermal annealing (RTA) furnace for 30 min in vacuum at a temperature of 530 °C [8,17]. The thickness of the grown samples was estimated to be ~112 nm by X-ray reflectivity measurements. The structural characterization of VO_2 thin film prepared on a m-Al_2O_3 substrate was studied using the BL5A beamline of Pohang Light source-II, Pohang, Republic of Korea. X-rays of 11.57 keV were used to obtain synchrotron X-ray diffraction (XRD) measurements, and the obtained data were converted to Cu K_α energy to be shown in the present manuscript. The surface morphology of the prepared sample was studied by atomic force microscopy (AFM) using the Veeco Dimension 3100 SPM instrument (Veeco Instruments Inc. 112 Robin Hill Road Santa Barbara CA 93117, Goleta, CA, USA) at room temperature. The Raman spectrum was obtained using a micro-Raman spectrometer (Witec Alpha 300 RA, Ulm, Germany) with a 532 nm wavelength and a 1 μm spot size for the laser excitation. The temperature-dependent resistance of VO_2 thin film grown on the m-Al_2O_3 substrate was measured using the Keithley 2612B (Keithley, Cleveland, OH, USA) source-meter in terms of four-probe geometry. X-ray absorption (XAS) measurements at V *K*-edge were performed in the fluorescence mode measured using the 8C beamline of the Pohang Light Source II (PLS II). XAS measurements at V *L*-edge and O *K*-edge in the total electron yield (TEY) mode were taken using the 2A MS undulator beamline of Pohang Light source-II, Pohang, Republic of Korea.

3. Results

The surface topography and surface roughness of the VO_2/m-Al_2O_3 film analyzed by using the AFM image are shown in Figure 1a,b, respectively. The surface of the grown film is quite homogenous and continuous. In the AFM image, the nano-scale granular surface is evident, and the root mean square (RMS) roughness is estimated to be ~1.2 nm. The RMS roughness value in the present sample is significantly lower than that of the recently reported epitaxial VO_2 film on an m-Al_2O_3 substrate [15]. Room temperature Raman spectra of the VO_2/m-Al_2O_3 thin film sample and bare m-Al_2O_3 substrate are shown in Figure 1c. The observed Raman modes at 141 cm^{-1}, 194 cm^{-1}, 224 cm^{-1}, 309 cm^{-1}, and 611 cm^{-1} are in good agreement with the earlier reports on VO_2, and this advocates the monoclinic M1 phase of VO_2 in the current sample [14–16,18–20]. Figure 1d shows the room temperature synchrotron XRD data (measured in θ–2θ geometry) of the VO_2 film deposited on the m-Al_2O_3 substrate. Apart from the substrate peak in the XRD data, a single diffraction peak appearing at ~64.87° in the film corresponding to the ($\bar{4}02$) plane of the monoclinic M1 phase of VO_2 is observed. Further, no other phase peak was detected in

the XRD data of the grown sample, indicating the epitaxial growth of the monoclinic M_1 phase of VO_2 on the m-Al_2O_3 substrate. The epitaxial relationship between the VO_2 film and the m-Al_2O_3 substrate was further examined with Φ-scans (Figure 1e) of the off-axis planes of VO_2 and the substrate. The off-axis $(11\bar{2}0)$ plane peak of the m-Al_2O_3 substrate exhibits a two rotational symmetry, with 180° in Φ-scan. The off-axis $(\bar{2}11)$ plane peak of VO_2 exhibits a four-fold rotational symmetry with 90°, confirming the epitaxial relationship between the VO_2 thin film and m-Al_2O_3 substrate.

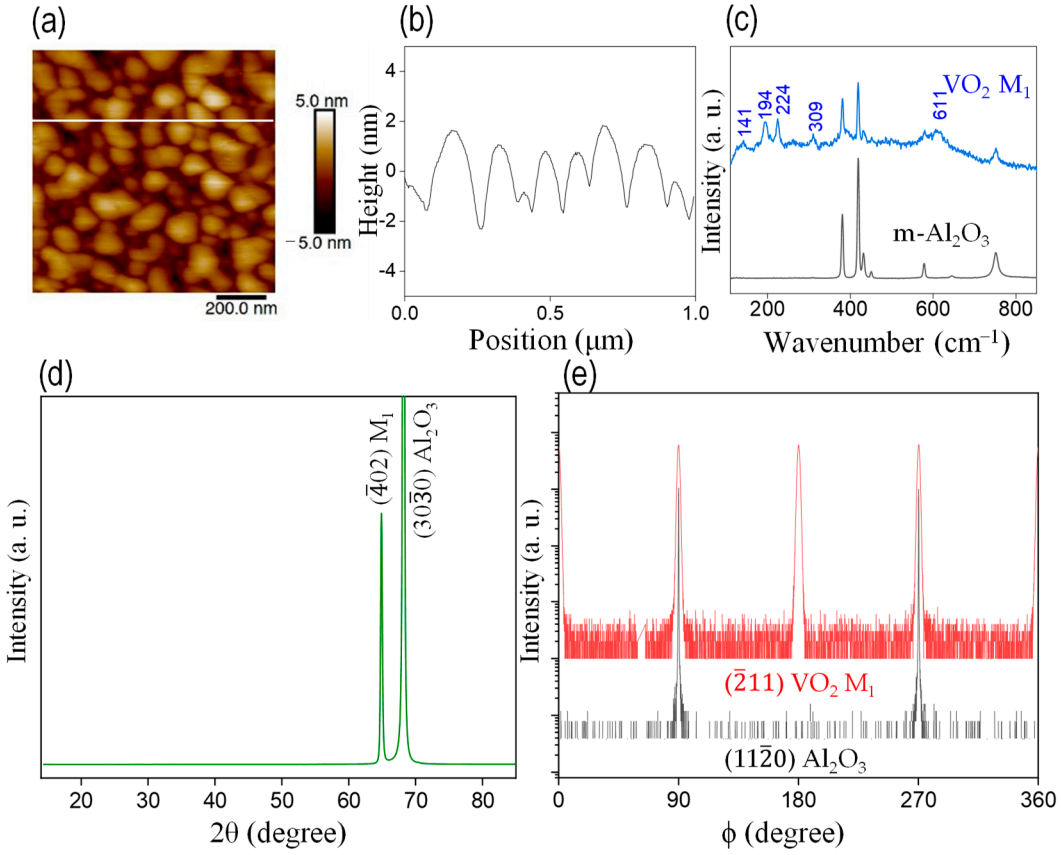

Figure 1. (**a**) AFM image of the VO_2/m-Al_2O_3 thin film sample at room temperature. (**b**) The height profile for the white line position in AFM image shown in (**a**). (**c**) Room temperature Raman spectra of bare m-Al_2O_3 substrate and VO_2/m-Al_2O_3 thin film. (**d**) Room temperature θ–2θ XRD profile of VO_2/m-Al_2O_3 thin film. (**e**) Off-axis $(\bar{2}11)$ plane (at Ψ = 32.36°) of VO_2 thin film shows the four-fold symmetry in Φ-scan, and the off-axis $(11\bar{2}0)$ plane (at Ψ = 44.99°) of m-Al_2O_3 substrate shows the two-fold symmetry in Φ-scan.

Temperature-dependent XRD measurements in the θ–2θ geometry were further carried out at several temperatures at a range of 31 °C–90 °C in order to check the monoclinic M_1 → rutile structural phase transition in the VO_2/m-Al_2O_3 thin film sample. The measured temperature-dependent XRD data are shown in Figure 2a,b for the thermal cycles of heating and cooling, respectively. During heating, the $(\bar{4}02)$ plane peak of the monoclinic M_1 phase of VO_2 remains stable below 53 °C. During further heating, an additional peak corresponding to the (002) plane peak of the rutile VO_2 phase emerges at a higher 2θ value. At a temperature of 68 °C and above, the $(\bar{4}02)$ plane peak of the monoclinic M_1 phase disappears. The observed behavior of the $(\bar{4}02)$ plane and (002) plane peaks in the temperature-dependent XRD data signifies the monoclinic M_1 → rutile structural phase transition in the VO_2 thin film sample. The reversibility of this structural phase transition is checked by taking temperature-dependent XRD measurements during the cooling cycle, as shown in Figure 2b. Upon cooling, the $(\bar{4}02)$ plane peak of the monoclinic M_1 phase

starts to reappear at ~60 °C, and a rutile → monoclinic M_1 structural phase transition was witnessed.

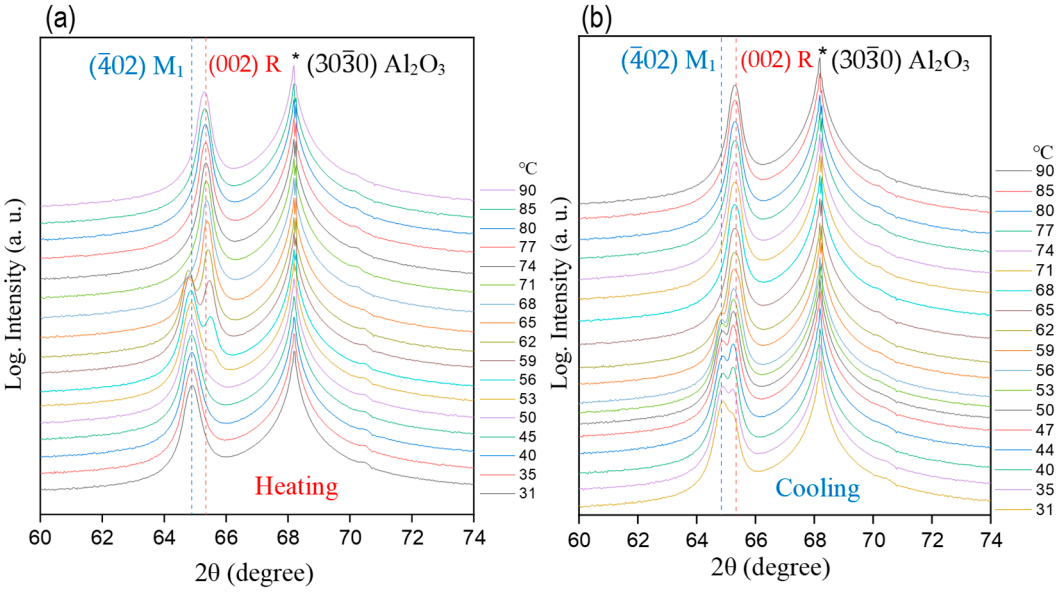

Figure 2. XRD spectra of VO_2 thin film prepared on m-Al_2O_3 substrate during (**a**) heating and (**b**) cooling cycles. Substrate peaks are marked as * in these figures.

The contour plots of the temperature-dependent XRD data during the heating and cooling cycles are together plotted in Figure 3 to display the reversible nature of the monoclinic $M_1 \longleftrightarrow$ rutile structural phase transition in the VO_2 thin film sample. The transformation of the (4̄02) M_1 diffraction peak to (002) R during heating, and vice versa, during cooling is clearly visible. Moreover, the structural phase transition temperature is lower in the cooling cycle as compared to that during the heating cycle, representing a hysteresis associated with first-order phase transition.

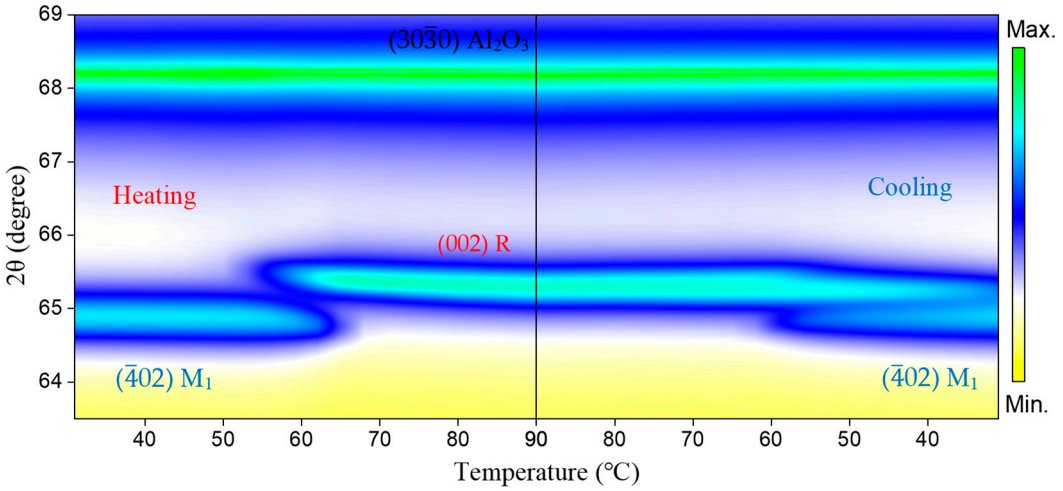

Figure 3. The contour plot of the temperature-dependent XRD data. In this plot, XRD intensities are plotted as functions of temperature (horizontal axes) and diffraction angle 2θ (vertical axes) values.

Figure 4a shows the normalized resistance (R (T)/R (T = 27 °C)) of the VO_2 film sample as a function of temperature during the heating and cooling cycles, while Figure 4b depicts the temperature derivative of the resistance. In the studied temperature range, a four-order change in resistance is seen for the VO_2 thin film prepared on the m-Al_2O_3

substrate, and the abrupt changes in resistance are associated with the MIT transition. The VO_2 thin film behaves as an insulator at room temperature and becomes metallic above the electrical transition temperature. Hysteresis among the resistance curves during heating and cooling was also noticed. This thermal hysteresis is associated with the latent heat of the first-order phase transition, which is driven by the microstructure of the thin film [21]. The electrical transition temperatures observed during the heating and cooling cycles are 68 °C and 59.5 °C, respectively. The MIT temperature (during the heating cycle) for the current epitaxial VO_2 thin film sample is close to that of single crystal VO_2 [22]. Earlier, Zhao et al. reported an MIT temperature of 64.5 °C with a thermal hysteresis width of 6.1 °C for the VO_2 thin film grown on the m-Al_2O_3 substrate with a mixed orientation [14].

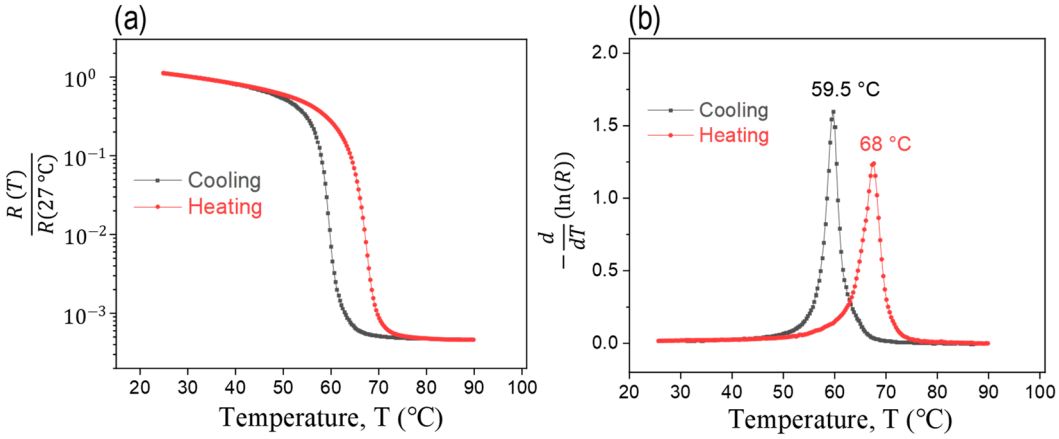

Figure 4. (**a**) Temperature-dependent normalized resistance (R(T)/R(27 °C)) of VO_2 thin film. (**b**) Temperature derivative of the resistance curves during heating and cooling cycles.

In order to obtain further insights on the crystal structure and the electronic structure of the VO_2/m-Al_2O_3 thin film sample, XAS measurements were carried out. Figure 5a shows the V *K*-edge XANES (X-ray absorption near edge spectroscopy) spectrum of the VO_2 thin film sample measured at room temperature. The spectral shape of the studied sample is similar to that of the XANES spectra of the VO_2 samples reported previously [8,17,23].

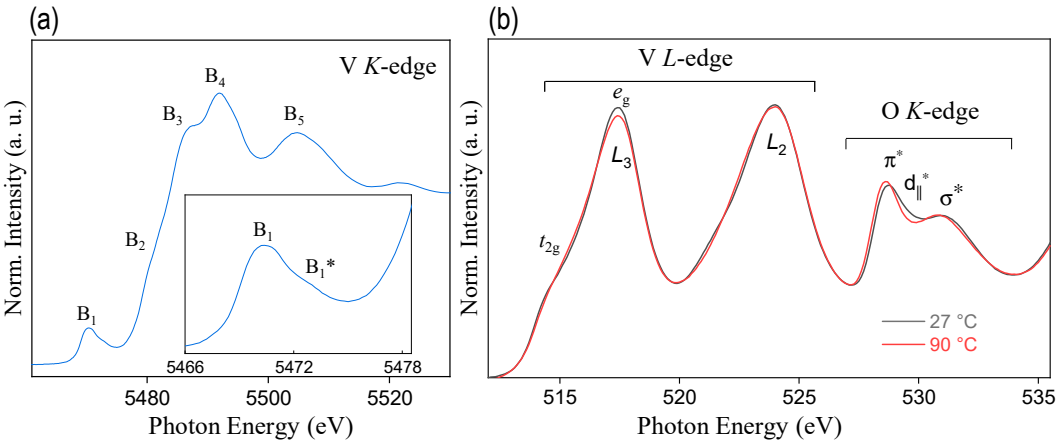

Figure 5. (**a**) Normalized XANES spectrum measured at V *K*-edge for VO_2 thin film sample at room temperature. Inset of (**a**) shows the enlarged view of the XANES spectrum around the pre-edge region. (**b**) X-ray absorption spectra recorded in TEY mode at V *L*-edge and O *K*-edge at different temperatures.

As per earlier reports, six distinct features, namely B_1, B_1*, B_2, B_3, B_4, and B_5, can be assigned to the XANES spectrum of the VO_2 thin film sample. It is well known that the

pre-edge peak gives information about the geometry of the absorber atom [24–26]. The inset of Figure 5a depicts the enlarged view of the pre-edge region. In monoclinic M_1 phase of VO_2, pre-edge spectra are characterized by two peaks, B_1 and B_1^*. Features B_1 and B_1^* arise due to 1s → 3*d* (V)/2*p* (O) transitions, which are mainly t_{2g} (B_1) and e_g (B_1*) in character [26]. Feature B_1^* appears in the insulating monoclinic M_1 phase of VO_2 and is suppressed in the metallic rutile phase of VO_2. Therefore, the spectral features in the room-temperature XANES spectrum point to the stoichiometry of the VO_2 thin film sample with the +4 oxidation state of V and confirm the monoclinic M1 phase at room temperature. V *L*-edge and O *K*-edge XAS spectra were further recorded at 27 °C and 90 °C (Figure 5b) in order to study the electronic structure changes in the insulating monoclinic M_1 phase and metallic rutile phase of the VO_2 thin film. In the room-temperature XAS spectrum, the spectral features at ~518 eV and ~524 eV belongs to the L_3 and L_2 edges of V, respectively. V 2*p* core-level (spin-orbit split $2p_{3/2}$ and $2p_{1/2}$) transition into the unoccupied V 3*d* states are responsible for these spectral features [8,27]. The additional features in the V *L*-edge at ~515.7 eV and ~522.3 eV originate due to the transitions to the crystal-field-split t_{2g} part of the V 3*d* states [8,17]. Based on the existing literature, the spectral features in the O *K*-edge XAS spectrum appearing around ~529.6eV, 530.4 eV, and 532.2 eV can be linked to transitions into the π^*, $d_{||}^*$, and σ^* hybridization band, respectively [8,17,27,28]. The shape and energy positions of the spectral features observed in V *L*-edge and O *K*-edge XAS spectrum (at 27 °C), as well as the spin orbit splitting values of the L_3 and L_2 edges of V, are consistent with the earlier report of VO_2 single crystal and thin films [8,28–30].

The lowest conduction band (π^*) in the O *K*-edge XAS spectrum accounts for the conductivity of the material, while the $d_{||}^*$ band stipulates the structural distortion and is related with the V-V dimerization along the rutile c axis [31,32]. The $d_{||}^*$ states are associated with V-V dimerization in the low-temperature-insulating phase, and therefore, these are considered to be a fingerprint of the monoclinic M_1 structure. These $d_{||}^*$ states are likely to become suppressed in the rutile metallic phase of VO_2 due to the absence of V-V dimers. As expected, the $d_{||}^*$ states disappear in the XAS spectrum recorded at 90 °C. Additionally, a shift of π^* states towards a lower photon energy value is seen at 90 °C, indicating the metallic nature of VO_2 thin film at this temperature. So, the spectral feature changes in the O *K*-edge XAS spectrum measured below and above the MIT temperature are very well correlated to the temperature-dependent structural and electrical changes in the VO_2 thin film prepared on the m-Al_2O_3 substrate.

4. Conclusions

In summary, VO_2 thin film was prepared on an m-Al_2O_3 substrate using a RF magnetron sputtering technique, and its uniform coverage on the substrate was confirmed by AFM. The room-temperature monoclinic M_1 phase of the grown VO_2 film was established through Raman and synchrotron XRD measurements. Phi-scan measurements confirmed the epitaxial growth of VO_2 on the m-Al_2O_3 substrate. The VO_2 thin film displays a monoclinic M_1 → rutile structural phase transition at ~68 °C. The MIT transition in VO_2 thin film was also noticed at ~68 °C. The reversible nature of the structural phase transition and electrical transition was seen in the temperature-dependent XRD and electrical resistance measurements, respectively, during the heating and cooling cycles. XAS spectra at the V *K*-edge, V *L*-edge, and O *K*-edge further confirm the monoclinic M_1 phase and stoichiometry of the VO_2 thin film sample at room temperature. Moreover, the O *K*-edge XAS spectrum depicts a shifting of the π^* states towards lower photon energy values, and the suppression of $d_{||}^*$ states at 90 °C signifies the existence of a metallic rutile phase in the VO_2 thin film at this temperature.

Author Contributions: Data curation, M.K. and S.R.; Methodology, M.K., S.R. and H.H.L.; writing—original draft preparation, M.K. and S.R.; writing—review and editing, M.K. and H.H.L. supervision, H.H.L.; funding acquisition, H.H.L. All authors have read and agreed to the published version of the manuscript.

Funding: This work was supported by the National Research Foundation of Korea (NRF) grants funded by the Korean government (MSIT) (Grant No. NRF-2021R1A2C1095669). SR-XRD measurements at PLS-II (Pohang Light Source II, POSTECH) were supported in part by MSIT, Korea.

Institutional Review Board Statement: Not applicable.

Informed Consent Statement: Not applicable.

Data Availability Statement: The data that support the findings of this study are available from the corresponding author upon reasonable request.

Acknowledgments: The authors acknowledge Anupam Giri for the technical help with taking the Raman measurements.

Conflicts of Interest: The authors declare no conflict of interest.

References

1. Shi, R.; Shen, N.; Wang, J.; Wang, W.; Amini, A.; Wang, N.; Cheng, C. Recent Advances in Fabrication Strategies, Phase Transition Modulation, and Advanced Applications of Vanadium Dioxide. *Appl. Phys. Rev.* **2019**, *6*, 11312. [CrossRef]
2. Kumar, M.; Kim, Y.; Lee, H.H. Temperature Dependent Structural, Electrical and Electronic Investigation of VO_2 (B) Thin Film. *Curr. Appl. Phys.* **2021**, *30*, 85–90. [CrossRef]
3. Kumar, M.; Singh, S.; Lim, W.C.; Chae, K.H.; Lee, H.H. Effect of Implantation of Nitrogen Ions into VO_2 Thin Films. *Mater. Lett.* **2022**, *310*, 131438. [CrossRef]
4. Saharan, C.; Rana, P.S.; Kumar, M. Phase Transition and Optical Properties of VO_2 and Al: ZnO/VO_2 Thin Films. *Coatings* **2022**, *12*, 1737. [CrossRef]
5. Kumar, M.; Rani, S.; Lee, H.H. Effect of Ti:ZnO Layer on the Phase Transition and the Optical Properties of VO_2 Film. *J. Korean Phys. Soc.* **2019**, *75*, 519–522. [CrossRef]
6. Cui, Y.; Ke, Y.; Liu, C.; Chen, Z.; Wang, N.; Zhang, L.; Zhou, Y.; Wang, S.; Gao, Y.; Long, Y. Thermochromic VO_2 for Energy-Efficient Smart Windows. *Joule* **2018**, *2*, 1707–1746. [CrossRef]
7. Morin, F.J. Oxides Which Show a Metal-to-Insulator Transition at the Neel Temperature. *Phys. Rev. Lett.* **1959**, *3*, 34–36. [CrossRef]
8. Kumar, M.; Rani, S.; Pal Singh, J.; Hwa Chae, K.; Kim, Y.; Park, J.; Hwi Lee, H. Structural Phase Control and Thermochromic Modulation of VO_2 Thin Films by Post Thermal Annealing. *Appl. Surf. Sci.* **2020**, *529*, 147093. [CrossRef]
9. Liu, K.; Lee, S.; Yang, S.; Delaire, O.; Wu, J. Recent Progresses on Physics and Applications of Vanadium Dioxide. *Mater. Today* **2018**, *21*, 875–896. [CrossRef]
10. Yang, Z.; Ko, C.; Ramanathan, S. Oxide Electronics Utilizing Ultrafast Metal-Insulator Transitions. *Annu. Rev. Mater. Res.* **2011**, *41*, 337–367. [CrossRef]
11. Zhang, Y.; Xiong, W.; Chen, W.; Zheng, Y. Recent Progress on Vanadium Dioxide Nanostructures and Devices: Fabrication, Properties, Applications and Perspectives. *Nanomaterials* **2021**, *11*, 338. [CrossRef]
12. Kumar, M.; Saharan, C.; Rani, S. Thin Film Stabilization of Different VO_2 Polymorphs. In *Thin Films*; IntechOpen: London, UK, 2020. [CrossRef]
13. Katase, T.; Endo, K.; Ohta, H. Thermopower Analysis of Metal-Insulator Transition Temperature Modulations in Vanadium Dioxide Thin Films with Lattice Distortion. *Phys. Rev. B* **2015**, *92*, 35302. [CrossRef]
14. Zhao, Y.; Hwan Lee, J.; Zhu, Y.; Nazari, M.; Chen, C.; Wang, H.; Bernussi, A.; Holtz, M.; Fan, Z. Structural, Electrical, and Terahertz Transmission Properties of VO_2 Thin Films Grown on c-, r-, and m-Plane Sapphire Substrates. *J. Appl. Phys.* **2012**, *111*, 53533. [CrossRef]
15. Choi, Y.; Lee, D.; Song, S.; Kim, J.; Ju, T.-S.; Kim, H.; Kim, J.; Yoon, S.; Kim, Y.; Phan, T.B.; et al. Correlation between Symmetry and Phase Transition Temperature of VO_2 Films Deposited on Al_2O_3 Substrates with Various Orientations. *Adv. Electron. Mater.* **2021**, *7*, 2000874. [CrossRef]
16. Liang, W.; Gao, M.; Lu, C.; Zhang, Z.; Chan, C.H.; Zhuge, L.; Dai, J.; Yang, H.; Chen, C.; Park, B.H.; et al. Enhanced Metal–Insulator Transition Performance in Scalable Vanadium Dioxide Thin Films Prepared Using a Moisture-Assisted Chemical Solution Approach. *ACS Appl. Mater. Interfaces* **2018**, *10*, 8341–8348. [CrossRef]
17. Kumar, M.; Singh, J.P.; Chae, K.H.; Park, J.; Lee, H.H. Annealing Effect on Phase Transition and Thermochromic Properties of VO_2 Thin Films. *Superlattices Microstruct.* **2020**, *137*, 106335. [CrossRef]
18. Wu, Y.F.; Fan, L.L.; Chen, S.M.; Chen, S.; Zou, C.W.; Wu, Z.Y. Spectroscopic Analysis of Phase Constitution of High Quality VO_2 Thin Film Prepared by Facile Sol-Gel Method. *AIP Adv.* **2013**, *3*, 42132. [CrossRef]
19. Chouteau, S.; Mansouri, S.; Mohamedou, M.L.O.N.; Chaillou, J.; Suleiman, A.O.; le Drogoff, B.; Chaker, M. Investigation of the Metal-to-Insulator Transition of N-Doped $VO_2(M_1)$ Thin Films. *Appl. Surf. Sci.* **2021**, *554*, 149661. [CrossRef]
20. Shvets, P.; Dikaya, O.; Maksimova, K.; Goikhman, A. A Review of Raman Spectroscopy of Vanadium Oxides. *J. Raman Spectrosc.* **2019**, *50*, 1226–1244. [CrossRef]
21. Narayan, J.; Bhosle, V.M. Phase Transition and Critical Issues in Structure-Property Correlations of Vanadium Oxide. *J. Appl. Phys.* **2006**, *100*, 103524. [CrossRef]

22. Mun, B.S.; Chen, K.; Leem, Y.; Dejoie, C.; Tamura, N.; Kunz, M.; Liu, Z.; Grass, M.E.; Park, C.; Yoon, J.; et al. Observation of Insulating–Insulating Monoclinic Structural Transition in Macro-Sized VO_2 Single Crystals. *Phys. Status Solidi (RRL)—Rapid Res. Lett.* **2011**, *5*, 107–109. [CrossRef]
23. Majid, S.S.; Sahu, S.R.; Ahad, A.; Dey, K.; Gautam, K.; Rahman, F.; Behera, P.; Deshpande, U.; Sathe, V.G.; Shukla, D.K. Role of V-V Dimerization in the Insulator-Metal Transition and Optical Transmittance of Pure and Doped VO_2 Thin Films. *Phys. Rev. B* **2020**, *101*, 014108. [CrossRef]
24. Kumar, M.; Singh, J.P.; Chae, K.H.; Kim, J.H.; Lee, H.H. Structure, Optical and Electronic Structure Studies of Ti:ZnO Thin Films. *J. Alloys Compd.* **2018**, *759*, 8–13. [CrossRef]
25. Bianconi, A. Multiplet Splitting of Final-State Configurations in x-Ray-Absorption Spectrum of Metal VO_2 Effect of Core-Hole-Screening, Electron Correlation, and Metal-Insulator Transition. *Phys. Rev. B* **1982**, *26*, 2741–2747. [CrossRef]
26. Marini, C.; Pascarelli, S.; Mathon, O.; Joseph, B.; Malavasi, L.; Postorino, P. Tracking Competitive Lattice Distortions in Strongly Correlated VO_2-Based Systems: A Temperature-Dependent EXAFS Study. *Europhys. Lett.* **2013**, *102*, 66004. [CrossRef]
27. Haverkort, M.W.; Hu, Z.; Tanaka, A.; Reichelt, W.; Streltsov, S.V.; Korotin, M.A.; Anisimov, V.I.; Hsieh, H.H.; Lin, H.J.; Chen, C.T.; et al. Orbital-Assisted Metal-Insulator Transition in VO_2. *Phys. Rev. Lett.* **2005**, *95*, 4–7. [CrossRef]
28. Abbate, M.; de Groot, F.M.F.; Fuggle, J.C.; Ma, Y.J.; Chen, C.T.; Sette, F.; Fujimori, A.; Ueda, Y.; Kosuge, K. Soft-x-Ray-Absorption Studies of the Electronic-Structure Changes through the VO_2 Phase Transition. *Phys. Rev. B* **1991**, *43*, 7263–7266. [CrossRef]
29. Gray, A.X.; Jeong, J.; Aetukuri, N.P.; Granitzka, P.; Chen, Z.; Kukreja, R.; Higley, D.; Chase, T.; Reid, A.H.; Ohldag, H.; et al. Correlation-Driven Insulator-Metal Transition in Near-Ideal Vanadium Dioxide Films. *Phys. Rev. Lett.* **2016**, *116*, 116403. [CrossRef] [PubMed]
30. Aetukuri, N.B.; Gray, A.X.; Drouard, M.; Cossale, M.; Gao, L.; Reid, A.H.; Kukreja, R.; Ohldag, H.; Jenkins, C.A.; Arenholz, E.; et al. Control of the Metal-Insulator Transition in Vanadium Dioxide by Modifying Orbital Occupancy. *Nat. Phys.* **2013**, *9*, 661–666. [CrossRef]
31. Quackenbush, N.F.; Paik, H.; Wahila, M.J.; Sallis, S.; Holtz, M.E.; Huang, X.; Ganose, A.; Morgan, B.J.; Scanlon, D.O.; Gu, Y.; et al. Stability of the M2 Phase of Vanadium Dioxide Induced by Coherent Epitaxial Strain. *Phys. Rev. B* **2016**, *94*, 085105. [CrossRef]
32. Kumar, S.; Strachan, J.P.; Pickett, M.D.; Bratkovsky, A.; Nishi, Y.; Williams, R.S. Sequential Electronic and Structural Transitions in VO observed Using X-Ray Absorption Spectromicroscopy. *Adv. Mater.* **2014**, *26*, 7505–7509. [CrossRef] [PubMed]